Long Noncoding RNA UCA1 Promotes Glutamine-Driven Anaplerosis of Bladder Cancer by Interacting With hnRNP I/L to Upregulate GPT2 Expression

Hua Zhao
The First Affiliated Hospital of Xi'an Jiaotong University
Wenjing Wu
The First Affiliated Hospital of Xi'an Jiaotong University
Xu Li
The First Affiliated Hospital of Xi'an Jiaotong University
Wei Chen (chenweixjtu808@gmail.com)
The First Affiliated Hospital of Xi'an Jiaotong University

Research

Keywords: UCA1, hnRNP, lncRNA, Glutamine-driven anaplerosis, metabolism, bladder cancer

Posted Date: December 29th, 2020

DOI: https://doi.org/10.21203/rs.3.rs-135604/v1

Version of Record: A version of this preprint was published at Translational Oncology on March 1st, 2022. See the published version at https://doi.org/10.1016/j.tranon.2022.101340.

Abstract

Background: Glutamine-driven anaplerosis maintains the tricarboxylic acid (TCA) cycle by replenishing its carbon source of intermediates with the glutamine-derived carbons in cancer cells. Long noncoding RNA urothelial cancer associated 1 (UCA1), initially identified in bladder cancer, is associated with multiple cellular processes, including metabolic reprogramming. However, its characteristics in the anaplerosis context of bladder cancer (BLCA) remains elusive.

Methods: The mechanism of UCA1 bound to and facilitated the combination of hnRNP I/L to the promoter of GPT2 gene was investigated by RNA pulldown, qRT-PCR, western blot, dual luciferase reporter assays, immunohistochemical staining, chromatin immunoprecipitation and chromatin isolation by RNA purification. Metabolomics analysis and metabolic flux analysis were conducted to assess the effects of UCA1, hnRNP I/L, and GPT2 on metabolic reprogramming of BLCA.

Results: We identified UCA1 as a binding partner of heterogeneous nuclear ribonucleoproteins (hnRNPs) I and L, RNA-binding proteins with no previously known role in metabolic reprogramming. UCA1 and hnRNP I/L profoundly affected glycolysis, TCA cycle, glutaminolysis, and viability of BLCA cells. Importantly, UCA1 specifically bound to and facilitated the combination of hnRNP I/L to the promoter of glutamic pyruvate transaminase 2 (GPT2) gene, resulting in upregulated expression of GPT2 and enhanced glutamine-derived carbons in the TCA cycle. We also systematically confirmed the influence of UCA1, hnRNP I/L, and GPT2 on metabolism and proliferation via glutamine-driven anaplerosis in BLCA cells.

Conclusions: Our study reveals the critical mechanism by which UCA1 forms a functional UCA1-hnRNP I/L complex that upregulates GPT2 expression to promote glutamine-driven TCA cycle anaplerosis, providing novel evidence that lncRNA regulates metabolic reprogramming in tumor cells.

Background

Cancer cells reprogram their metabolism to fulfill anabolic and energetic requirements for survival and high proliferation. Enhanced uptake and utilization of glucose and glutamine is a prominent feature of cancer cells. Through aerobic glycolysis, or the Warburg effect, glucose is metabolized to lactate to generate energy rather than entering the tricarboxylic acid (TCA) cycle [1–4]. In addition to glycolysis, glutamine metabolism, or glutaminolysis, is another central route for anabolic metabolism and energy production. In cancer cells, the intermediates of the TCA cycle are also used as precursors for the synthesis of proteins, lipids, nucleic acids, and other biomolecules that are crucial to energy production and biosynthesis. The pool of intermediates in the TCA cycle must be replenished to maintain the TCA cycle function and balance the influx of metabolites, which is called anaplerosis [5, 6].

Glutamine-driven anaplerosis is the most common way to fuel the TCA cycle in rapidly proliferative cells [7]. As the most abundant amino acid in the mammalian body, glutamine is an essential source that provides proliferating cells with carbon and nitrogen for biosynthesis [8–10]. Glutamine is introduced into the cell by glutamine transporters, such as solute carrier family 1, member 5 (SLC1A5) and solute carrier family 7, member 5 (SLC7A5). Through glutaminolysis, glutaminase (GLS) hydrolyzes glutamine to glutamate, which is then converted to α-Ketoglutarate (α-KG) with the aid of glutamate oxaloacetate transaminase (GOT) or glutamate

pyruvate transaminase (GPT) or glutamate dehydrogenase (GLDH) [10–12]. Importantly, glutamine-derived α-KG serves as a critical anaplerotic substrate and carbon source for the TCA cycle in many cancers cells when TCA intermediates are used for biosynthetic precursors [13]. Glutaminolysis involved enzymes and glutamine transporters have been found dysregulated in cancers [14, 15].

Long non-coding RNAs (lncRNAs), a group of endogenous RNAs longer than 200 nt and lack protein-coding ability, can affect genes involved in cancer metabolism [16, 17]. LncRNA urothelial carcinoma associated 1 (UCA1), initially identified and highly upregulated in bladder cancer, is believed to function in tumorigenesis, development, as well as the metabolism of bladder cancer [16, 18]. However, the exact mechanism by which UCA1 promotes the metabolic reprogramming in bladder cancer cells remains unclear. For the tumorigenicity of UCA1, one mechanism worth mentioning is its capability of forming complexes with RNA-binding proteins (RBPs), including heterogeneous nuclear ribonucleoproteins (hnRNPs) which represent a large family of RBPs. HnRNPs assist in multiple cellular processes, such as alternative splicing, mRNA stabilization, and translation. Multiple hnRNPs play a crucial role in tumorigenesis, and their expression level is altered in various cancers [19, 20]. HnRNP I and L are striking among the hnRNPs family. HnRNP I is involved in regulating metabolic shift from oxidative phosphorylation to anaerobic glycolysis in many cancers [21–23]. Huang et al. [24] reported hnRNP I can interact with 19 lncRNAs in breast cancer cells, among which UCA1 is on the top of the list in terms of enrichment. The interaction of UCA1 with hnRNP I suppresses the p27 and regulates breast cancer cell growth. The RNA-binding capacity of hnRNPs is mediated by RNA recognition motifs (RRMs). All four RRMs were found with high sequence similarity and shared between hnRNP I and L [19, 25]. Therefore, it is likely that hnRNP I and L can interact with UCA1. But it still unclear whether UCA1 binds to hnRNP I/L and how they play a part in bladder cancer metabolism.

In this report, we demonstrated that UCA1, hnRNP I/L, and GPT2 were markedly overexpressed in bladder cancer tissues and cell lines and profoundly impacted bladder cancer metabolic reprogramming. Importantly, UCA1 bound specifically to hnRNP I/L and form a functional UCA1-hnRNP I/L complex that upregulated GPT2 expression by binding to its promoter and promote glutamine-driven TCA anaplerosis.

Methods

Clinical samples and study approval

Tissues were collected from patients who underwent surgery at the First Affiliated Hospital of Xi'an Jiaotong University, Xi'an, China. All patients were not treated with chemotherapy or radiotherapy before surgery. All samples were collected and used following the ethical policies of the institutional review board of the First Affiliated Hospital of Xi'an Jiaotong University. The clinical characteristics of bladder cancer patients are shown in Table 1.

Cell culture

Cell lines 5637, T24, UMUC2, and SV-HUC-1 were purchased from American Type Culture Collection and maintained in RPMI 1640 (containing 10% fetal bovine serum) unless otherwise stated. Stable cell lines with ectopic expression of UCA1 in UMUC2 cells (constructed with pcDNA3.1(+)/Mock and pcDNA3.1(+)/UCA1,

respectively), and cell lines with knockdown of UCA1 in 5637 cells (pRNAT-U6.1/Neo-shCtrl and pRNAT-U6.1/Neo-shUCA1, respectively) were constructed and selected in our laboratory.

Lentivirus transduction

To establish cell lines stably expressing shRNAs or genes, the pre-packaged lentivirus expressing shRNA or cDNA fragments of hnRNP I, hnRNP L, and GPT2 were purchased from GenePharma (Shanghai, China) and used to infect cells following the manufacturer's instructions. Cells were transduced with lentivirus to establish cell lines stably expressing shRNAs or genes, and selected by 1 μg/ml puromycin 2 days after infection. Stably infected pools were maintained in 1 μg/mL puromycin. Cells infected with viruses containing non-sense shRNA served as the control group. The transduction efficiency was validated by western blot analyses.

Western blotting

Block NC membrane was incubated overnight at 4°C with different primary antibodies: anti-hnRNP I (1:1000; Santa Cruz Biotechnology, Inc; CA, USA); anti-hnRNP L (1:1000; Santa Cruz Biotechnology, Inc; CA, USA); anti-GLS2 (1:1000); anti-GPT2 (1:1000; Abbacy, Cambridge, UK); anti-SLC1A5(1:500); anti-SLC7A5(1:500); anti-β actin (1:3000; CST; Beverly, MA, USA). After being washed, the membranes were incubated with HRP-conjugated goat-anti-mouse secondary antibodies (1:5000; Pierce; Rockford, IL, USA) for 1 hr at room temperature and visualized using Clarity™ Western ECL Substrate (Bio-Rad; Richmond, CA, USA).

Gene expression analysis

Total RNA was isolated with TRIzol reagent (Invitrogen, Carlsbad, CA, USA) or RNAFast200 (Fastagen, Shanghai, China) according to the manufacturer's protocol. RT-qPCR was performed following the instructions of PrimeScript RT Master Mix Kit and SYBR Premix Ex Taq Kit (Takara, Clontech, Kyoto, Japan) with CFX96 Touch Real-Time PCR Detection System (Bio-Rad, Hercules, CA, USA). The sequences of primers used for qPCR are listed in Table 2.

Cell viability assay

Cells (3.5×10^3 per well) were cultured in triplicate in 96-well plates to perform cell viability tests using Cell Count Kit (7Sea, Shanghai, China). After 24 hr, 48 hr, 72 hr, and 96 hr, 10 μl CCK-8 was added to each well, plates were shaken for 5 times, incubated for an additional 50min and measured by reading OD450 nm using an EnSpire Reader (PerkinElmer, USA).

Dual-luciferase reporter assay

Luciferase assays were performed using the Dual-Luciferase™ Reporter Assay System (Promega; Madison, WI, USA) according to the manufacturer's protocol. HnRNP I/L overexpressing cells and control cells were transfected with 0.1 μg reporter plasmids (pGL3-GLS2 promotor or pGL3-GPT2 promotor) and 0.01 μg internal control (Renilla plasmid) in 96-well plates utilizing X-treme GENE siRNA Transfection Reagent (Roche, Indianapolis, IN, USA). Cells were harvested and lysed for dual-luciferase reporter assay 48 h after transfection. Renilla luciferase plasmid served as normalization.

Immunohistochemistry

Immunohistochemical analysis for the protein expression was performed as previously described [26] using anti-hnRNP I (1:500; Santa Cruz Biotechnology, Inc; CA, USA) anti-hnRNP L (1:500; Santa Cruz Biotechnology, Inc; CA, USA) GPT2 (1:300; Abcam, Cambridge, MA, USA). Slides were incubated overnight at 4 °C, and immunostaining was performed with a SPlink Detection Kit and DAB (ZSBIO, Beijing, China). Stained slides were captured and imaged by microscopy. The image quantification was analyzed using ImageJ(1.52q) with the IHC Profiler plugin [27]. The staining intensity was graded as negative (0), low positive (1+), positive (2+), or high positive (3+).

RNA pull-down

RNA pull-down assays were performed using PierceTM Magnetic RNA-Protein Pull-Down Kit (#20164, Thermo Fisher Scientific, Waltham, MA, USA) according to the manufacture's protocol. The RNA fragments of the entire UCA1 sequence, deleted form, or mutant form, were synthesized by GenePharma (Shanghai, China). Biotinylated RNA was bound to streptavidin magnetic beads and then incubated with cell lysates. RNA-binding protein complexes were washed and eluted. The retrieved samples were heated (10 minutes, 95℃) and detected by western blot analysis.

Chromatin immunoprecipitation assay (ChIP)

ChIP experiments were performed using EZ-Magna ChIP^{TM} A/G Chromatin Immunoprecipitation Kit (#17-10086, Merck Millipore, Billerica, MA, USA) according to the manufacturer's procedures. Cells were fixed in 1% formaldehyde for 10 min at room temperature to crosslink UCA1 to DNA. Nuclei were isolated with 500 μl nuclear lysis buffer supplemented with 2.5 μl protease inhibitor cocktail II. Chromatin DNA was sonicated (8min total, AmpL 30%, pulse on 10 s, pulse off 30 s) and sheared to a length between 200 bp to 1000 bp. The sheared cross-linked chromatin was incubated and rotated with immunoprecipitating antibodies: anti-hnRNP I (1.2μg/reaction; Santa Cruz Biotechnology, Inc; CA, USA)), anti-hnRNP L (1μg/reaction; Santa Cruz Biotechnology, Inc; CA, USA), normal Mouse IgG (1μg/reaction) or anti-RNA Polymerase (1μg/reaction) overnight at 4 °C. Primers for ChIP-qPCR are listed in Table 2.

Chromatin isolation by RNA purification (ChIRP)

ChIRP was performed using EZ-Magna CHIRP^{TM} RNA Interactome Kit (#17-10495, Merck Millipore, Billerica, MA, USA) as previously described [28]. Biotin-labeled DNA probes against UCA1 were designed at singlemoleculefish.com and synthesized by GenePharma (Shanghai, China). Cells were crosslinked in 1% formaldehyde at room temperature for 10 minutes. Cross-linked cell lysates were sonicated (15min total, AmpL 30%, pulse on 10 s, pulse off 30 s) and sheared to 100–500 bp fragments at 4°C, and hybridized with biotinylated probes. Retrieved DNA was quantified with SYBR Green PCR Kit (Takara, Clontech, Kyoto, Japan) to measure the enrichment of GPT2 promoter. The probes and primers sequences used in the ChIRP assay are listed in Table 2.

Metabolomics and metabolic flux analysis with mass spectrometry

Cells (1 x 10^6) were plated on 100mm dishes in RPMI-based media for 6 hr. Withdrawn the medium from dishes, washed with PBS ×2, and changed to tracing media for an additional 24 hr. The media were transferred to pre-chilled Eppendorf tubes. Supernatant samples were isolated after centrifugation at 1000 rpm for 5 min

and frozen at -80 °C until analysis. Cells were transferred to pre-chilled Eppendorf tubes, washed with cold PBS ×2, and centrifuged and flash frozen in liquid nitrogen. Before metabolite derivatization, media samples were dried under nitrogen gas and frozen at -80 °C. Cells were resuspended in 600 µl cold (-40 °C) 50% aqueous methanol, inserted in dry ice for 30 min, and thawed samples at 4 °C. Then added 400 µl chloroform, vortexed for 30 s before centrifugation at 14,000 rpm for 10 min at 4 °C. The supernatant was transferred to new Eppendorf tubes, dried, and stored at -80 °C. Metabolomics profiling and metabolic flux analysis was performed on Shimadzu QP-2010 Ultra GC-MS with an injection temperature of 250 °C and injected volume of 1 µL. GC oven temperature started at 110 °C for 4 min, rising to 230 °C at 3 °C/min and to 280 °C at 20 °C /min with a final hold at this temperature for 2 min. GC flow rate with helium carrier gas was 50 cm/s. The GC column used was a 20 m x 0.25 mm x 0.25 mm Rxi-5ms. GC-MS interface temperature was 300 °C and (electron impact) ion source temperature was set at 200 °C, with 70 V ionization voltages. The mass spectrometer was set to scan m/z range 50-800, with 1 kV detector. GC-MS data were analyzed to determine isotope labeling and quantities of metabolites. Metabolites with baseline separated peaks were quantified based on total ion count peak area, using standard curves generated from running standards in the same batch of samples. To determine ^{13}C labeling, the mass distribution for known fragments of metabolites was extracted from the appropriate chromatographic peak. These fragments contained either the whole carbon skeleton of the metabolite, or lacked the alpha carboxyl carbon, or (for some amino acids) contained only the backbone minus the side-chain [29]. For each fragment, the retrieved data comprised mass intensities for the lightest isotopomer. These mass distributions were normalized and corrected for the natural abundance of heavy isotopes of the elements H, N, O, Si and C, using matrix-based probabilistic methods as described [30], and implemented in MATLAB. Labeling results were expressed as fractions of the particular compound containing isotopic label from the particular precursor.

Statistical analysis

Data are presented as means ± SD and are representative of at least three independent experiments. Differences between two groups were analyzed with the unpaired/paired Student's t test using GraphPad Prism 8 software. All reported differences are $P < 0.01$ unless otherwise stated. Details of each specific statistical analysis are indicated in the figure legends.

Results

High expression of UCA1 and hnRNP I/L in BLCA

To investigate the expression profiles of UCA1 and hnRNP I/L in human cancers, we analyzed the available gene expression dataset, Oncomine, and compared expression of UCA1 and hnRNP I/L across muti-cancer analyses. Rank for UCA1 and hnRNP I is in the top 5%, and hnRNP L is in the top 1%. Oncomine analysis showed that UCA1 and hnRNP I/L were highly expressed genes in BLCA compared with other cancers (Fig. 1A). We further detected UCA1 and hnRNP I/L expression in human uroepithelium cell line (SV-HUC-1) and three typical BLCA cells (UMUC2, T24, 5637) by qRT-PCR and found that UCA1 and hnRNP I/L expression was much higher in BLCA cells, especially 5637 cells (Fig. 1B). We performed qRT-PCR assays and immunohistochemical staining (IHC) in clinical tissue samples. We found that UCA1 and hnRNP I/L expression in BLCA tissues were higher than normal tumor-adjacent bladder tissues (Fig. 1C). Additionally, Pearson's correlations of UCA1 and

hnRNP I/L showed a positive correlation between UCA1 and hnRNP I/L (Fig. 1D). IHC results further validated the upregulation of hnRNP I/L in BLCA (Fig. 1E and F).

UCA1 interacts with hnRNP I/L

To further understand the relationship between UCA and hnRNP I/L, we first examined the effects of UCA1 knockdown and overexpression on hnRNP I/L. Results showed that hnRNP I/L is barely affected by UCA1 knockdown or overexpression (Fig. 2A and B). Conversely, 5637 BLCA cells stably expressing shRNAs against hnRNP I showed the downregulation of UCA1, and ectopic hnRNP I displayed the upregulation of UCA1 (Fig. 2C). Similar results were observed for hnRNP L (Fig. 2D). HnRNP I and L are striking RBPs and have been reported to interact with lncRNAs. We wonder whether UCA1 interacts with hnRNP I/L in BLCA. To verify this, we performed RNA pull down assays. Full-length UCA1 (1442 nt) and two truncated UCA1 (UCA1-1: 1-740 nt, UCA1-2: 741-1442 nt) were synthesized in vitro using T7 RNA polymerase and labeled with biotin. Those biotinylated RNA probes were used to pull down the 5637 cell lysates. Western blot analysis of hnRNP I/L in samples pulled down by biotinylated probes showed that the 5' term of UCA1 was responsible for the binding with hnRNP I/L (Fig. 2E). Within the UCA1-1 region, the 697-708 nt sequence (5'-CTCTTCCTCCTGG-3') is similar to hnRNP I binding motif CYYYYCYYY (Y/G) G, and the 209-214 nt sequence (5'-CACACA-3') is similar to CA-enriched hnRNP L binding motif (Fig. 2F, left). Thus, we synthesized two mutant UCA1-1 probes (UCA1-1 mt1: mutant from 697-708 nt; UCA1-1 mt2: mutant 209-214 nt) to perform pull down assays. HnRNP I/L in samples pulled down by wild type UCA1-1 and mutant UCAI-1 probes were analyzed by western blot, and the results showed that the motifs are essential for binding hnRNP I and hnRNP L (Fig. 2F, right). These results confirmed that UCA1 could form an RNP complex with hnRNP I/L.

UCA1 and hnRNP I/L affect BLCA metabolic reprogramming

We were interested in whether UCA1 and hnRNP I/L may affect BLCA cell metabolism. To investigate this, mass spectrometry (MS) analysis was utilized to measure multiple critical metabolites in the culture medium and cells. Increased glucose levels, decreased lactate levels, and increased glutamine levels were detected in the culture medium of UCA1 and hnRNP I/L knockdown cells (Fig. 3A-C, left). And decreased glucose levels, increased lactate levels, and increased glutamine levels were detected in the medium of UCA1 and hnRNP I/L overexpression cells (Fig. 3A-C, right). This suggested that the consumption of glucose and glutamine and secretion of lactate were increased by upregulated UCA1 and hnRNP I/L. MS also measured twelve critical metabolites in 5637 cells. Among these were glycolysis intermediates (3-PG and pyruvate), TCA cycle intermediates (citrate, α-KG, succinate, fumarate, and malate), intermediates of glutamine catabolism (glutamate and aspartate), and glucogenic amino acid (glycine, alanine, and serine). Results showed that UCA1 and hnRNP I/L knockdown significantly reduced these intermediates except serine and alanine (Fig. 3D, left). In comparison, overexpression of UCA1 and hnRNP I/L significantly increased these intermediates except serine and alanine (Fig. 3D, right).

To further explore the different metabolic responses to shUCA1, shhnRNP I, and shhnRNP L, we performed stable-isotope tracing experiments with glucose or glutamine labeled with ^{13}C (at all carbon atoms). Results showed that UCA1 knockdown did not affect the fraction of ^{13}C-glucose-derived carbon of α-KG, succinate,

fumarate, malate, glutamate, and asparate (Fig. 3E, left) and the fraction of ^{13}C-glutamine derived carbon of pyruvate, lactate, and alanine (Fig. 3F, right), but reduced the fraction of ^{13}C-glutamine derived carbon of citrate, α-KG, succinate, fumarate, malate, glutamate, and asparate (Fig. 3F, left) and the fraction ^{13}C-glucose-derived carbon of citrate, pyruvate, lactate, and alanine (Fig. 3E, right). HnRNP I knockdown did not affect the fraction of ^{13}C-glucose-derived carbon of citrate, α-KG, succinate, fumarate, malate, glutamate, asparate, and alanine (Fig. 3G) and the fraction of ^{13}C-glutamine derived carbon of asparate and alanine (Fig. 3H). However, it reduced the fraction of ^{13}C-glutamine derived carbon of citrate, α-KG, succinate, fumarate, malate, glutamate, pyruvate, and lactate (Fig. 3H) and the fraction of ^{13}C-glucose-derived carbon of pyruvate and lactate (Fig. 3G). HnRNP L knockdown had no effect on the fraction of ^{13}C-glucose-derived carbon of citrate, α-KG, succinate, fumarate, glutamate, asparate, and alanine (Fig. 3G) and the fraction of ^{13}C-glutamine derived carbon of fumarate, malate, asparate, and alanine (Fig. 3h), but reduced the fraction of ^{13}C-glutamine derived carbon of citrate, α-KG, succinate, malate, glutamate, pyruvate, and lactate (Fig. 3H) and the fraction of ^{13}C-glucose-derived carbon of malate, pyruvate, and lactate (Fig. 3G). Besides, we examined the effect of UCA1 and hnRNP I/L on cell viability. CCK8 assays revealed that UCA1 and hnRNP I/L downregulation significantly slowed cell viability (Fig. 3I, left), whereas downregulation of UCA1 and hnRNP I/L significantly accelerated cell viability (Fig. 3I, middle). Moreover, the addition of α-KG, citric, and malate (TCA cycle intermediates) in culture media could rescue the restrained proliferation induced by knockdown of UCA1, hnRNP I, and hnRNP L (Fig. 3I, right). In contrast to BLCA cancer cells, UCA1 and hnRNP I/L knockdown cells downregulated glutamine-derived anaplerosis and glycolysis (Fig. 3J). These results imply that UCA1 and hnRNP I/L, which upregulated in BLCA, significantly impact cell metabolic reprogramming, especially in replenishing TCA cycle intermediates by upregulating glutamine anaplerosis.

UCA1 regulates GPT2 expression by interacting with hnRNP I/L

Glucose and glutamine are the two most essential fuels for cancer cell proliferation and growth. 5637 cells were able to proliferate in complete or glucose-free RPMI 1640 medium (10% FBS) medium, whereas unable to proliferate in glutamine-free or both glutamine-free and glucose-free RPMI 1640 medium (10% FBS), suggesting that 5637 cells required glutamine more than glucose for proliferation (Fig. 4A). Then we were interested in investigating how UCA1 and hnRNP I/L reprogram the glutamine metabolism of BLCA cells. First, we used qRT-PCR to evaluate whether UCA1 and hnRNP I/L regulate important genes involved in the glutaminolysis of 5637 cells. Next, western blot was performed to assess the relationship between the changed genes and UCA1 or hnRNP I/L (Fig. 4B-D). The results showed that SLC1A5 and SLC7A5 were positively related to UCA1 but not affected by hnRNP I/L. GLS2 and GPT2 were positively related to both UCA1 and hnRNP I/L. Also,dual-luciferase reporter assay showed that upregulated hnRNP I or L significantly increased luciferase activity of GPT2 promoter-pGL3 reporter vector (Fig. 4E), but not affected GLS2 promoter-pGL3 reporter vector (Data not shown).

Because UCA1 and hnRNP I/L could form RNP complex, and analysis of GPT2 promoter found hnRNP I/L binding sequences, we hypothesized that UCA1 and hnRNP I/L might regulate GPT2 gene expression by forming a complex at the promotor of GPT2 gene. ChIPassays revealed that hnRNP I/L bound to the promoter of GPT2 gene and knockdown of UCA1 or hnRNP I/L decreased the binding of hnRNP I/L to GPT2 promoter

region (Fig. 4F). CHIRP assays indicated that UCA1 is associated with the sequence of GPT2 promoter (Fig. 4G). Overexpression of UCA1 showed no effect on GPT2 expression in hnRNP I/L knockdown cells (Fig. 4H), which further confirmed that UCA1 and hnRNP I/L collaboratively regulated the transcriptional activity of GPT2.As a supplement, we validated the significant upregulation and positive correlation between GPT2 and UCA1 or hnRNP I/L in clinical BLCA tissues (Fig. 4I-K). These results demonstrated that UCA1 and hnRNP I/L formed a complex that regulated GPT2 expression by binding to the GPT2 promotor.

The role of GPT2 in glutamate-driven anaplerosis

We then investigated the role of GPT2 in BLCA metabolism reprogramming. Critical metabolites in culture medium and cells were detected by MS analysis. Also, ^{13}C-glucose and ^{13}C-glutamine tracing with MS were used to observe differential fractions of labeled carbon in glutamate and TCA cycle intermediates in metabolic pathways. In the culture medium of GPT2-knockdown 5637 cells, we observed increased glucose levels, decreased lactate levels, and increased glutamine levels (Fig. 5A, left), which meant the GPT2 knockdown suppressed the consumption of glucose and glutamine and secretion of lactate. GPT2-knockdown 5637 cells exhibited significantly decreased levels of several critical metabolites, including glycolysis intermediates (3-PG and pyruvate), TCA cycle intermediates (citrate, α-KG, succinate, fumarate, and malate), but did not affect intermediates of glutamine catabolism (glutamate and aspartate) and glucogenic amino acid (glycine, alanine, and serine) (Fig. 5A, right). Furthermore, ^{13}C-tracing experiments showed that GPT2 knockdown did not affect glucose contribution to TCA cycle intermediates and glutamine contribution to glycolysis intermediates, but suppressed glutamine contribution to TCA cycle intermediates and glucose contribution to glycolysis intermediates (Fig. 5B). GPT2-knockdown 5637 cells showed the inhibition to supply glutamine-derived metabolites for the TCA cycle or to maintain glycolysis. Insistently, suppressed 5637 cell proliferation induced by GPT2 knockdown (Fig. 5C, left) could be rescued by TCA cycle intermediates (α-KG, citrate, and malate) (Fig. 5C, right). Together these findings suggest that GPT2 is crucial for glutamate-driven anaplerosis that fueled the TCA cycle function in highly proliferative 5637 cells.

Discussion

Here, we report a previously uncharacterized mechanism by which UCA1, combining with hnRNP I/L, contributes to the metabolic reprogramming of bladder cancer. We observed that UCA1 and hnRNP I/L were markedly upregulated and positively correlated in bladder cancer. They formed a ribonucleoprotein complex and affect bladder cancer cell metabolism and viability via glutamine metabolism. Significantly, the UCA1-hnRNP I/L complex was involved in the glutamine-driven TCA anaplerosis of bladder cancer by binding with the GPT2 promoter. These observations complement our previous studies that linking UCA1 to dysregulated cancer metabolism, reveal the mechanism of UCA1 involved in glutamine-driven TCA cycle anaplerosis, and provide a novel experimental basis of lncRNA regulating metabolic reprogramming in tumor cells.

The regulatory roles of LncRNAs in dysregulated cancer metabolism exert through diverse mechanisms, particularly in regulating glucose, glutamine, and mitochondrial function [17, 31, 32]. As for UCA1, several mechanisms of regulating metabolism in bladder cancer have been demonstrated. It stimulates glycolysis indirectly through activating the mTOR-STAT3 pathway and inhibiting microRNA-143 expression to upregulate

the expression of hexokinase 2 [33]. UCA1 promotes glutaminolysis through interferes with the negative regulation of GLS2 mRNA by microRNA-16 to upregulate GLS2 expression and inhibits ROS production to protect cells from oxidative toxicity in bladder cancer [34, 35]. UCA1 acts as a competing endogenous RNA to inhibit microRNA-195, resulting in elevated ARL2 expression, which is essential for mitochondrial activity in bladder cancer [26]. Herein, our results show that the downregulation of UCA1 plays metabolic inhibition roles, including glucose and glutamine metabolism, suggesting that UCA1 gets potential clinical translation for bladder cancer via the regulation of cancer metabolism. We also observed a similar negative effect on the metabolic profile with the downregulation of hnRNP I/L (Fig. 3). Given the RNA stabilization function of hnRNP I/L [19, 20, 36, 37] and their combination with UCA1 (Fig. 2), it is likely that hnRNP I/L may affect metabolism at least partially through increasing the UCA1 stability, which explains the similar metabolic profiles.

Glutamine-driven anaplerosis, another step beyond the Warburg effect, is required for oncogene-induced tumorigenesis and metabolic reprogramming in many cancer cells [5, 38–40]. Despite the increasing evidence implicating the vital role of UCA1 in cancer metabolism, it has been poorly characterized in the anaplerosis context of bladder cancer. As pointed out earlier, glutamine can function in anaplerotic reactions through glutaminolysis. Metabolic enzymes are often found to be targeted by lncRNAs directly or indirectly in cancers. In this study, we observed that bladder cancer cells required glutamine, rather than glucose, for survival. And glutaminolytic enzymes GLS2 and GPT2 expression were upregulated by UCA1, hnRNP I, and hnRNP L. Besides, glutamine transporter SLC1A5 and SLC7A5 were upregulated by UCA1, not hnRNP I/L, and the mechanism needs to be further clarified. Significantly, UCA1 and hnRNP I/L form a functional RNP complex, which could activate the expression of GPT2 by binding to its promoter region. In consistent with these results, stable-isotope tracing experimental data showed a profound suppression of glutamine-driven carbons contributing to the TCA cycle by knockdown of UCA1, hnRNP I, hnRNP L, and GPT2. Therefore, our findings uncover a novel mechanism for UCA1 in glutamine-driven anaplerosis and complement previous studies linking UCA1 to bladder cancer glutamine metabolism [34].

The role of UCA1 in the interaction of hnRNP I/L with GPT2 promoter is an interesting paradigm. HnRNP I/L are known for their post-transcriptional regulation activities that control mRNA splicing, stability, and translation [19, 41]. However, recent studies have indicated that lncRNAs interact with hnRNP I or L to function in transcriptional regulation. Linc1992 interacts with hnRNP L and binds to regulate TNFα expression [42]. LncLGR forms a functional complex with hnRNP L to facilitates the recruitment of hnRNP L to the glucokinase promoter in fasted mice [43]. Our study indicated the role of UCA1, hnRNP I/L, and GPT2 in metabolic reprogramming, especially in glutamine-driven anaplerosis. And our data do not rule out the possibility that UCA1 or hnRNP I/L may regulate GPT2 expression by other unidentified pathways or cellular factors. Intriguingly, the impact of UCA1 and hnRNP I/L on glutamine-driven anaplerosis strongly suggests that they may also contribute to other metabolic processes. And their mechanism in regulating cancer metabolic reprogramming will emerge in the future.

Conclusions

Together, our work shows that UCA1 and hnRNP I/L exhibit substantial effects on bladder cancer metabolic reprogramming and reveals the unexpected mechanism of UCA1 forming a functional UCA1-hnRNP I/L complex that upregulates GPT2 expression to promote glutamine-driven TCA anaplerosis.

Abbreviations

UCA1: urothelial cancer associated 1; BLCA: bladder cancer; hnRNPs: heterogeneous nuclear ribonucleoproteins; lncRNAs: long non-coding RNAs; α-KG: α-Ketoglutarate; GPT2: glutamic pyruvate transaminase 2; SLC1A5: solute carrier family 1, member 5; SLC7A5: solute carrier family 7, member 5; GLS: glutaminase; GOT: glutamate oxaloacetate transaminase; GPT: glutamate pyruvate transaminase; GLDH: glutamate dehydrogenase; RRMs: RNA recognition motifs; IHC: immunohistochemical staining; MS: mass spectrometry; 3-PG: D-glycerate 3-phosphate.

Declarations

Ethics approval and consent to participate

The clinical samples were collected after informed consent was obtained. Studies were performed with the approval of the medical ethics committee of the First Affiliated Hospital of Xi'an Jiaotong University.

Consent for publication

Not applicable.

Availability of data and materials

All data generated or analysed during this study are included in this published article and are available from the corresponding author upon reasonable request.

Competing interests

The authors declare no conflicts of interest.

Funding

This study was supported by grants from the National Natural Science Foundation of China (Grant NO. 81772735).

Authors' contributions

HZ performed the experiments and wrote the article; HZ, WJ, and WC conceived and designed the experiments; WC and XL contributed reagents/materials/analysis tools. WC, XL, and WJ revised the paper. All authors read and approved the final manuscript.

Acknowledgements

Not applicable.

References

1. Devic S. Warburg Effect - a Consequence or the Cause of Carcinogenesis? J Cancer. 2016;7:817–22.

2. Zhao Y, Wang D, Xu T, Liu P, Cao Y, Wang Y, et al. Bladder cancer cells re-educate TAMs through lactate shuttling in the microfluidic cancer microenvironment. Oncotarget. 2015;6:39196–210.
3. Seyfried TN, Flores RE, Poff AM, D'Agostino DP. Cancer as a metabolic disease: implications for novel therapeutics. Carcinogenesis. 2014;35:515–27.
4. Ghaffari P, Mardinoglu A, Nielsen J. Cancer Metabolism: A Modeling Perspective. Front Physiol. 2015;6:1–9.
5. Ochoa-Ruiz E, Diaz-Ruiz R. Anaplerosis in cancer: Another step beyond the warburg effect. Am J Mol Biol. 2012;02:291–303.
6. Owen OE, Kalhan SC, Hanson RW. The key role of anaplerosis and cataplerosis for citric acid cycle function. J Biol Chem. 2002;277:30409–12.
7. Cluntun AA, Lukey MJ, Cerione RA, Locasale JW. Glutamine Metabolism in Cancer: Understanding the Heterogeneity. Trends in cancer. 2017;3:169–80.
8. Medina MA. Glutamine and cancer. J Nutr. 2001;131:2539S-42S.
9. Chambers JW, Maguire TG, Alwine JC. Glutamine metabolism is essential for human cytomegalovirus infection. J Virol. 2010;84:1867–73.
10. Son J, Lyssiotis CA, Ying H, Wang X, Hua S, Ligorio M, et al. Glutamine supports pancreatic cancer growth through a KRAS-regulated metabolic pathway. Nature. 2013;496:101–5.
11. Otter SJ, Chatterjee J, Stewart AJ, Michael A. The Role of Biomarkers for the Prediction of Response to Checkpoint Immunotherapy and the Rationale for the Use of Checkpoint Immunotherapy in Cervical Cancer. Clin Oncol. 2019;31:834–43.
12. Li T, Le A. Glutamine Metabolism in Cancer. Adv Exp Med Biol. 2018;1063:13–32.
13. DeBerardinis RJ, Lum JJ, Hatzivassiliou G, Thompson CB. The biology of cancer: metabolic reprogramming fuels cell growth and proliferation. Cell Metab. 2008;7:11–20.
14. Cao Y, Lin SH, Wang Y, Chin YE, Kang L, Mi J. Glutamic pyruvate transaminase GPT2 promotes tumorigenesis of breast cancer cells by activating sonic hedgehog signaling. Theranostics. 2017;7:3021–33.
15. Sreedhar A, Zhao Y. Dysregulated metabolic enzymes and metabolic reprogramming in cancer cells. Biomed reports. 2018;8:3–10.
16. Lin W, Zhou Q, Wang CQ, Zhu L, Bi C, Zhang S, et al. LncRNAs regulate metabolism in cancer. Int J Biol Sci. 2020;16:1194–206.
17. Fan C, Tang Y, Wang J, Xiong F, Guo C, Wang Y, et al. Role of long non-coding RNAs in glucose metabolism in cancer. Mol Cancer. 2017;16:1–11.
18. Wang F, Li X, Xie X, Zhao L, Chen W. UCA1, a non-protein-coding RNA up-regulated in bladder carcinoma and embryo, influencing cell growth and promoting invasion. FEBS Lett. 2008;582:1919–27.
19. Geuens T, Bouhy D, Timmerman V. The hnRNP family: insights into their role in health and disease. Hum Genet Springer Berlin Heidelberg. 2016;135:851–67.
20. Hung L-H, Heiner M, Hui J, Schreiner S, Benes V, Bindereif A. Diverse roles of hnRNP L in mammalian mRNA processing: a combined microarray and RNAi analysis. RNA. 2008;14:284–96.

21. Zhu W, Zhou B, lun, Rong L, juan, Ye L, Xu H, Zhou Y, et al. Roles of PTBP1 in alternative splicing, glycolysis, and oncogensis. J Zhejiang Univ Sci B. 2020;21:122–36.
22. Minami K, Taniguchi K, Sugito N, Kuranaga Y, Inamoto T, Takahara K, et al. MiR-145 negatively regulates Warburg effect by silencing KLF4 and PTBP1 in bladder cancer cells. Oncotarget. 2017;8:33064–77.
23. Sugiyama T, Taniguchi K, Matsuhashi N, Tajirika T, Futamura M, Takai T, et al. MiR-133b inhibits growth of human gastric cancer cells by silencing pyruvate kinase muscle-splicer polypyrimidine tract-binding protein 1. Cancer Sci. 2016;107:1767–75.
24. Huang J, Zhou N, Watabe K, Lu Z, Wu F, Xu M, et al. Long non-coding RNA UCA1 promotes breast tumor growth by suppression of p27 (Kip1). Cell Death Dis. 2014;5:e1008.
25. Han SP, Tang YH, Smith R. Functional diversity of the hnRNPs: past, present and perspectives. Biochem J. 2010;430:379–92.
26. Li HJ, Sun XM, Li ZK, Yin QW, Pang H, Pan JJ, et al. LncRNA UCA1 Promotes Mitochondrial Function of Bladder Cancer via the MiR-195/ARL2 Signaling Pathway. Cell Physiol Biochem. 2017;43:2548–61.
27. Varghese F, Bukhari AB, Malhotra R, De A. IHC Profiler: an open source plugin for the quantitative evaluation and automated scoring of immunohistochemistry images of human tissue samples. PLoS One. 2014;9:e96801.
28. Chu C, Quinn J, Chang HY. Chromatin isolation by RNA purification (ChIRP). J Vis Exp. 2012;e3912.
29. Nanchen A, Fuhrer T, Sauer U. Determination of metabolic flux ratios from ^{13}C-experiments and gas chromatography-mass spectrometry data: protocol and principles. Methods Mol Biol. 2007;358:177–97.
30. van Winden WA, Wittmann C, Heinzle E, Heijnen JJ. Correcting mass isotopomer distributions for naturally occurring isotopes. Biotechnol Bioeng. 2002;80:477–9.
31. Lu W, Cao F, Wang S, Sheng X, Ma J. LncRNAs. The Regulator of Glucose and Lipid Metabolism in Tumor Cells. Front Oncol. 2019;9:1–11.
32. Xiao ZD, Zhuang L, Gan B. Long non-coding RNAs in cancer metabolism. BioEssays. 2016;38:991–6.
33. Li Z, Li X, Wu S, Xue M, Chen W. Long non-coding RNA UCA1 promotes glycolysis by upregulating hexokinase 2 through the mTOR-STAT3/microRNA143 pathway. Cancer Sci. 2014;105:951–5.
34. Li H-J, Li X, Pang H, Pan J-J, Xie X-J, Chen W. Long non-coding RNA UCA1 promotes glutamine metabolism by targeting miR-16 in human bladder cancer. Jpn J Clin Oncol. 2015;45:1055–63.
35. D'Autréaux B, Toledano MB. ROS as signalling molecules: mechanisms that generate specificity in ROS homeostasis. Nat Rev Mol Cell Biol. 2007;8:813–24.
36. Arake De Tacca LM, Pulos-Holmes MC, Floor SN, Cate JHD. PTBP1 mRNA isoforms and regulation of their translation. Rna. 2019;25:1324–36.
37. Hui J, Reither G, Bindereif A. Novel functional role of CA repeats and hnRNP L in RNA stability. Rna. 2003;9:931–6.
38. Wise DR, Thompson CB. Glutamine addiction: a new therapeutic target in cancer. Trends Biochem Sci. 2010;35:427–33.
39. Chen Q, Kirk K, Shurubor YI, Zhao D, Arreguin AJ, Shahi I, et al. Rewiring of Glutamine Metabolism Is a Bioenergetic Adaptation of Human Cells with Mitochondrial DNA Mutations. Cell Metab. 2018;27:1007–25.

40. Zhao Y, Zhao X, Chen V, Feng Y, Wang L, Croniger C, et al. Colorectal cancers utilize glutamine as an anaplerotic substrate of the TCA cycle in vivo. Sci Rep. 2019;9:19180.
41. Kishore S, Luber S, Zavolan M. Deciphering the role of RNA-binding proteins in the post-transcriptional control of gene expression. Brief Funct Genomics. 2010;9:391–404.
42. Li Z, Chao TC, Chang KY, Lin N, Patil VS, Shimizu C, et al. The long noncoding RNA THRIL regulates TNFα expression through its interaction with hnRNPL. Proc Natl Acad Sci U S A. 2014;111:1002–7.
43. Ruan X, Li P, Cangelosi A, Yang L, Cao H. A Long Non-coding RNA, lncLGR, Regulates Hepatic Glucokinase Expression and Glycogen Storage during Fasting. Cell Rep. 2016;14:1867–75.

Tables

Table 1. Characteristics of bladder cancer patients.

Characteristic	Patient frequency
Total	43
Gender	
Male	35 (81.4%)
Female	8 (18.6%)
Age	66 (34-85)
<66	21 (48.8%)
≥66	22 (51.2%)
Tumor stage	
T1	14 (32.6%)
T2-T4	29 (67.4%)
TNM stage	
I	14 (32.6%)
II	14 (32.6%)
III	7 (16.3%)
IV	8 (18.6%)

Table 2. Oligonucleotides sequences (5'->3')

qRCR primers (5'->3')		
UCA1	Forward	CTCTCCATTGGGTTCACCATTC
	Reverse	GCGGCAGGTCTTAAGAGATGAG
hnRNP I	Forward	AATGACAAGAGCCGTGACTAC
	Reverse	GGAAACCAGCTCCTGCATAC
hnRNP L	Forward	TTGTGGCCCTGTCCAGAGAATT
	Reverse	GTTTGTGTAGTCCCAAGTATCCTG
SLC1A5	Forward	GACCGTACGGAGTCGAGAAG
	Reverse	GGGGGTTTCCTTCCTCAGTG
SLC7A5	Forward	GAAGGCACCAAACTGGATGT
	Reverse	GAAGTAGGCCAGGTTGGTCA
GLS2	Forward	TGCCTATAGTGGCGATGTCTCA
	Reverse	GTTCCATATCCATGGCTGACAA
GPT2	Forward	GGAGCTAGTGACGG CATTTCTACGA
GPT2 promotor	Reverse	CCCAGGGTTGATTATGCAGAGCA
	Forward	CCTCCCCTGTCCCTACTGAT
	Reverse	ATGTCCATGCAGTCCCTTGC
β-actin	Forward	TCCCTGGAGAAGAGCTACGA
	Reverse	AGCACTGTGTTGGCGTACAG
GAPDH	Forward	GTCGGAGTCAACGGATTTG
	Reverse	TGGGTGGAATCATATTGGAA
shRNA		
UCA1	CCGGGTTAATCCAGGAGACAAAGACTCGAGTCTTTGTCTCCTGGATTAACTTTTTG	
hnRNP I	CCGGGCGTGAAGATCCTGTTCAATACTCGAGTATTGAACAGGATCTTCACGCTTTTTG	
hnRNP L	CCGGCCTCAACAACAACTTCATGTTCTCGAGAACATGAAGTTGTTGTTGAGGTTTTTG	
GPT2	CCGGGACAACGTGTACTCTCCAGATCTCGAGATCTGGAGAGTACACGTTGTCTTTTTG	

Control	CCGGTTCTCCGAACGTGTCACGTCTCGAGACGTGACACGTTCGGAGAATTTTTG
CHIRP probes	
Probe 1	aagggttgtaggttgtttgt
Probe 2	cggcaggtcttaagagatga
Probe 3	gttttagacttttgacccag
Probe 4	atatgcgtgtactgttgtcc
Probe 5	ccaagccctctaacaacaaa
Probe 6	gcagatcctatgcagaagag
Probe 7	aatagtattccctgttgcta
Probe 8	aatgtaggtggcgatgagtt

Figures

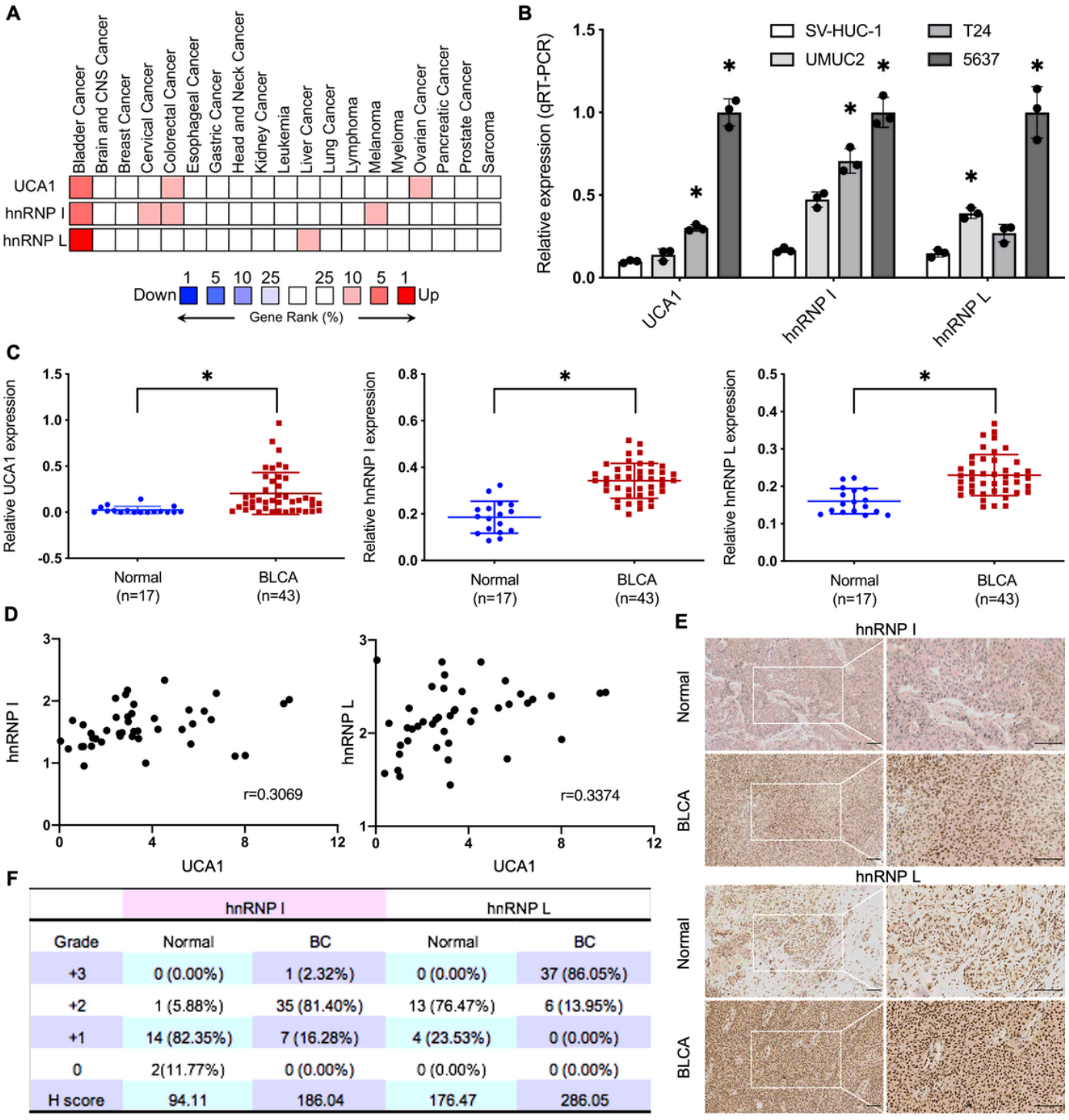

	hnRNP I		hnRNP L	
Grade	Normal	BC	Normal	BC
+3	0 (0.00%)	1 (2.32%)	0 (0.00%)	37 (86.05%)
+2	1 (5.88%)	35 (81.40%)	13 (76.47%)	6 (13.95%)
+1	14 (82.35%)	7 (16.28%)	4 (23.53%)	0 (0.00%)
0	2(11.77%)	0 (0.00%)	0 (0.00%)	0 (0.00%)
H score	94.11	186.04	176.47	286.05

Figure 1

Expression of UCA1 and hnRNP I/L in BLCA. A, High expression of UCA1 and hnRNP I/ L in BLCA. Oncomine analysis of UCA1 and hnRNP I/L across muti-cancer analyses (www.oncomine.org). The rank for a gene is the median rank for that gene across each of the analyses. P < 0.0001; Fold change > 2; 10% gene rank. B, High expression of UCA1 and hnRNP I/L in BLCA cells. One human uroepithelium cell and three BLCA cells were measured by qRT-PCR. n=3 independent experiments. C to F, High expression of UCA1 and hnRNP I/L in BLCA tissues: qRT-PCR of UCA1 and hnRNP I/L (C) was performed using normal tumor-adjacent bladder tissues

(n=17) and BLCA tissues (n=43), and Pearson's correlations of UCA1 and hnRNP I/L (D) were calculated; IHC of hnRNP I and hnRNP L (E) were performed using clinical tissues and H score (F) were determined. * P<0.01.

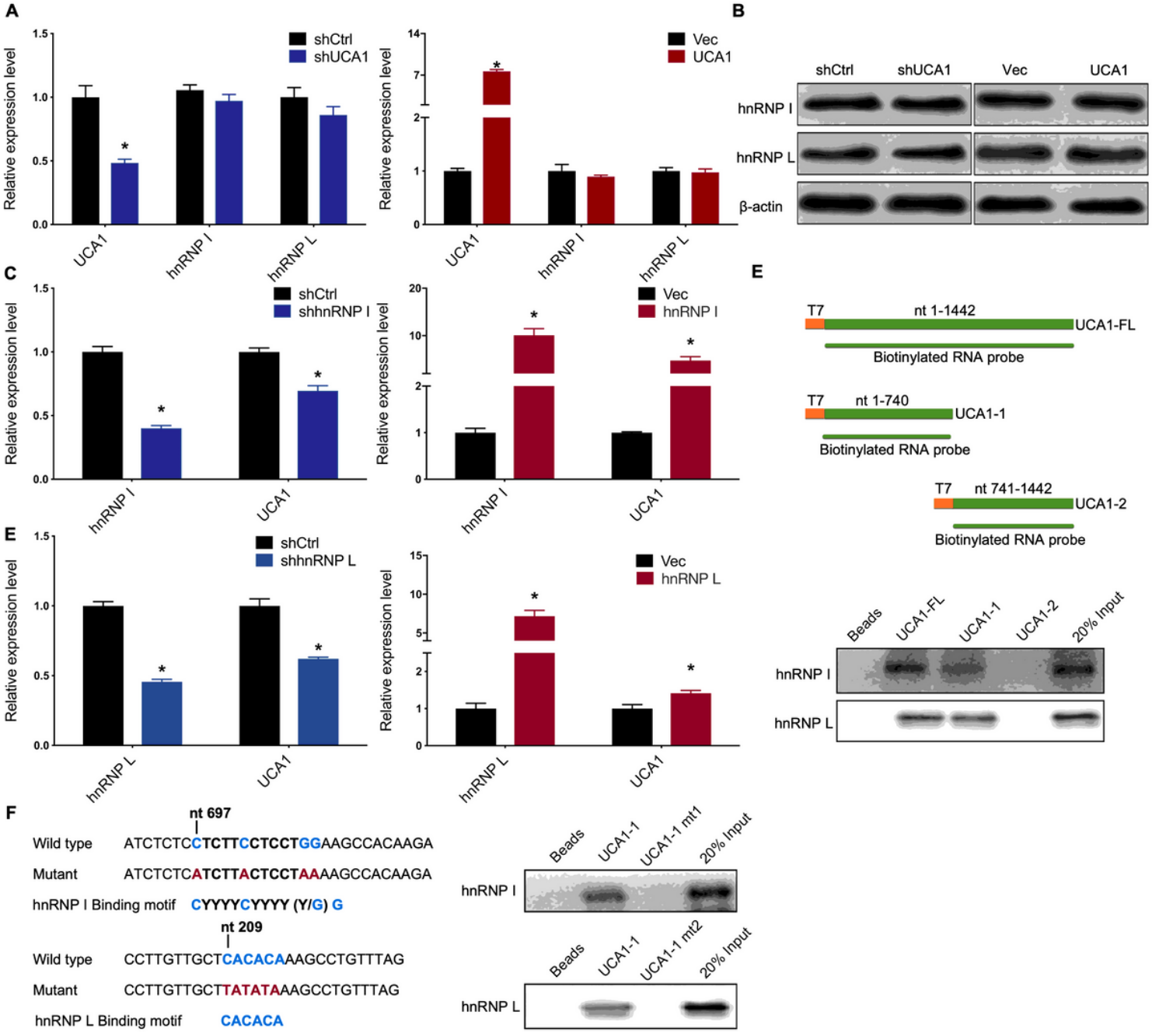

Figure 2

UCA1 is an hnRNP I/L binding partner. A, B, No effects of UCA1 on hnRNP I/L expression in BLCA cells. hnRNP I/L expression was analyzed in UCA1 knockdown (left) and UCA1 overexpression (right) BLCA cells by qRT-PCR (A) and western blot (B). C, D, Correlation between hnRNP I/L and UCA1 expression in BLCA cells. UCA1 expression was analyzed by qRT-PCR. hnRNP I/L deletion decreases the expression of UCA1 in BLCA cells (right); Ectopic hnRNP I/L increases the expression of UCA1 in BLCA cells (right). *P< 0.01. E, F, RNA pulldown assays validation of UCA1-hnRNP I/L bound regions in 5637 cells. Biotinylated full-length UCA1 (UCA1-FL) probe or truncated UCA1 probes (UCA1-1 and UCA1-2) were incubated with 5637 cell lysates. HnRNP I/L in samples pulled down by streptavidin beads were analyzed using western blot (E). Two mutant UCA1-1 at the

hnRNP I /L peak binding regions were described. HnRNP I/L in samples pulled down by wild type UCA1-1 and UCAI-1 mt probes labelled with biotin were analyzed by western blot (F).

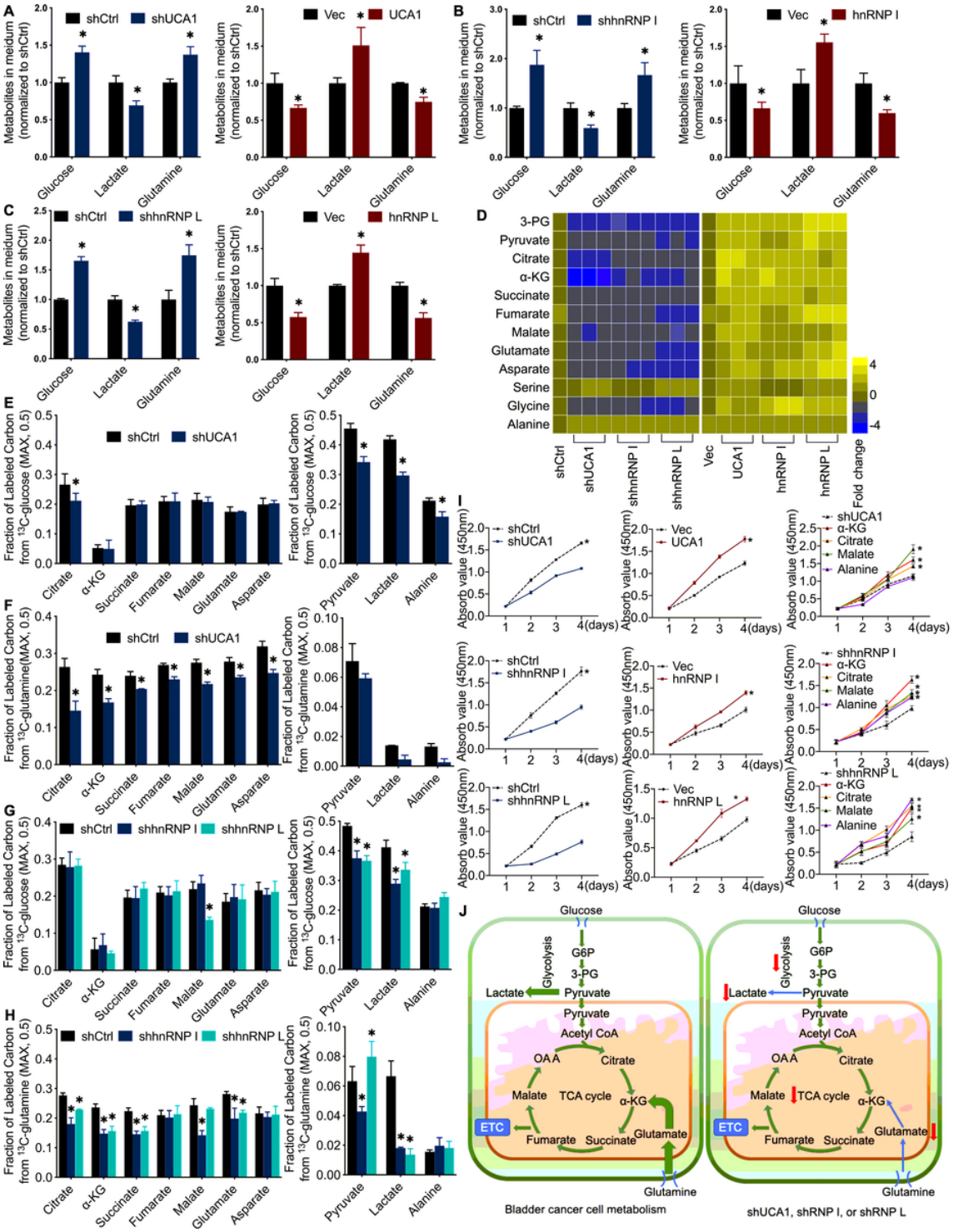

Figure 3

The Effect of UCA1, hnRNP I, and hnRNP L on cell metabolism in vitro. A to C, Glucose uptake, lactate secretion, and glutamine uptake decreased by UCA1 or hnRNP I/L knockdown in 5637 cells. Cells were grown in the medium for 24h, and levels of glucose, lactate, and glutamine in the medium were analyzed by MS and normalized to shCtrl group. * P < 0.01 compared with shCtrl group. D, Cellular Metabolites levels examined by MS and normalized to shCtrl group (n=3 independent experiments). E to H, Fraction of labelled metabolic

intermediates during 13C glucose (E-H, left) and 13C-glutamine (E-H, right) tracing experiments. I, α-KG, citrate, or malate rescues 5637 cells from suppressed cell proliferation caused by shUCA1, shhnRNP I, and shhnRNP L. Cells were grown in medium with the presence of the indicated nutrient. CCK8 assay was performed to determine the cell viability in 5637 cells for indicated times. n = 3 independent samples. *P < 0.01 compared with shCtrl group. J, Model depicting relative activity of fundamental metabolic pathways in 5637 bladder cancer cells (left), shUCA1, shhnRNP I, or shhnRNP L cells (right). 3-PG, D-glycerate 3-phosphate; G6P, glucose-6-phosphate; OAA, oxaloacetate; ETC, electron transport chain.

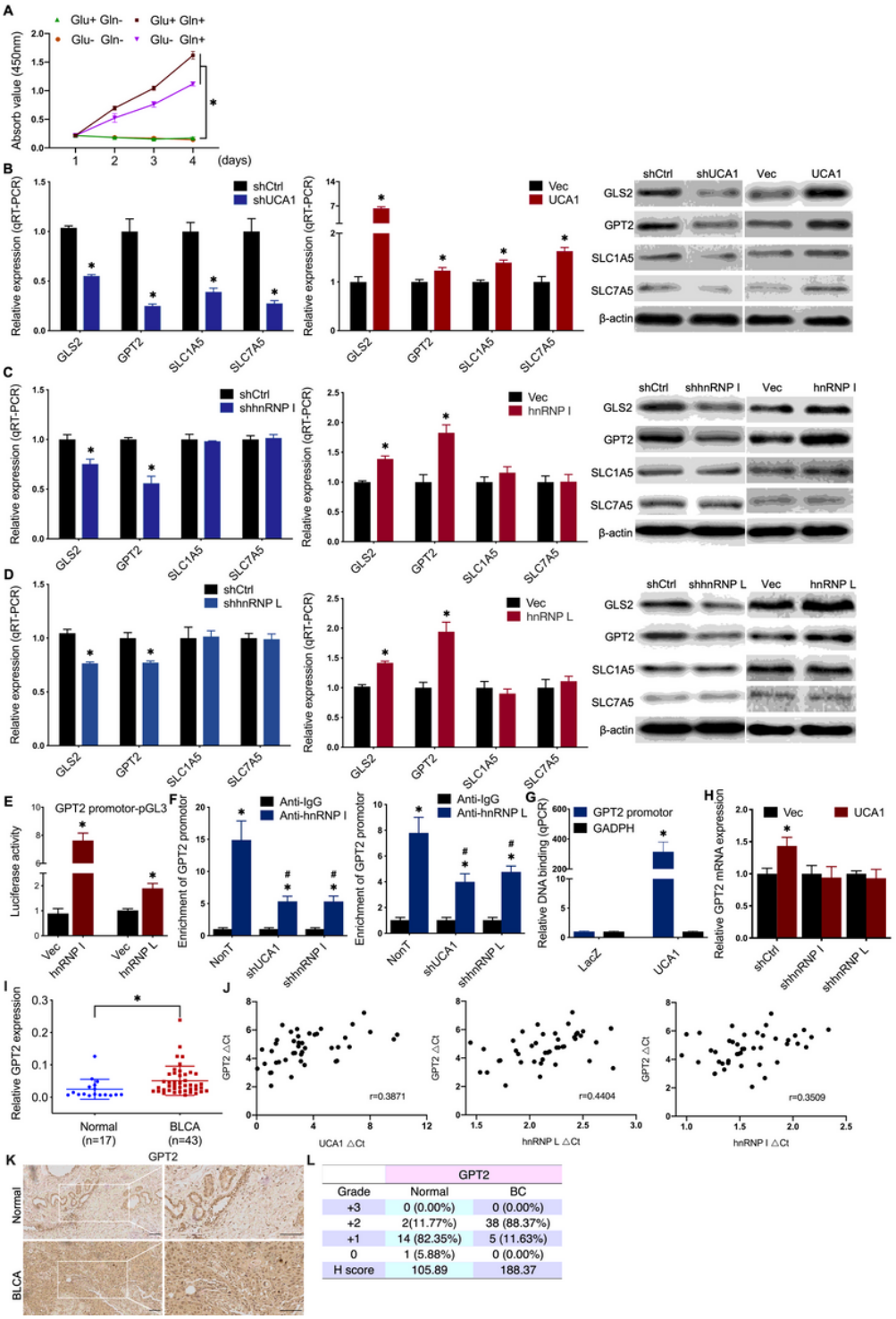

L

	GPT2	
Grade	Normal	BC
+3	0 (0.00%)	0 (0.00%)
+2	2(11.77%)	38 (88.37%)
+1	14 (82.35%)	5 (11.63%)
0	1 (5.88%)	0 (0.00%)
H score	105.89	188.37

Figure 4

UCA1 regulates GPT2 expression by interacting with hnRNP I/L A, Glutamine more than glucose was required for proliferation of 5637 cells. B to D, Screening of glutaminolysis associated enzymes: mRNA expression levels in UCA1 or hnRNP I/L knockdown (B to D, left) and UCA1 or hnRNP I/L overexpressed (B to D, middle) BLCA cells were analysed by qRT-PCR. Protein levels were detected by western blot (B to D, right). E, Activation of the GPT2 promotor-pGL3 reporter by hnRNP I/L. Luciferase activity under the control of the GPT2 promotor was normalized to constitutively expressed renilla luciferase in 293T cells transfected with control vector or hnRNP I/L plasmid. F, ChIP-qRCR detection of hnRNP I/L binding to the GPT2 promotor. Anti-IgA/G was used as the negative control. The fold enrichment of GPT2 promoter sequence in hnRNP I/L was normalized to IgA/G ChIP. *P < 0.01, compared with Anti-IgG; #P < 0.01 compared with NonT. G, CHIRP-qRCR detection of UCA1 binding to GPT2 promotor. UCA1 targeted probes and negative Lacz probes were used for ChIRP assay. The fold enrichment of GPT2 promotor or GADPH sequence in UCA1 CHIRP was normalized to LacZ CHIRP. *P < 0.01. H, Overexpression of UCA1 showed no effect on GPT2 expression in hnRNP I/L knockdown cells. *P < 0.01. I to L High expression of GPT2 in BLCA tissues: qRT-PCR of GPT2 (I) was performed using normal tumor-adjacent bladder tissues (n=17) and BLCA tissues (n=43), and Pearson’s correlations of GPT2 (J) were calculated; IHC of GPT2 (K) was performed using clinical tissues, and H score (L) was determined. * P<0.01

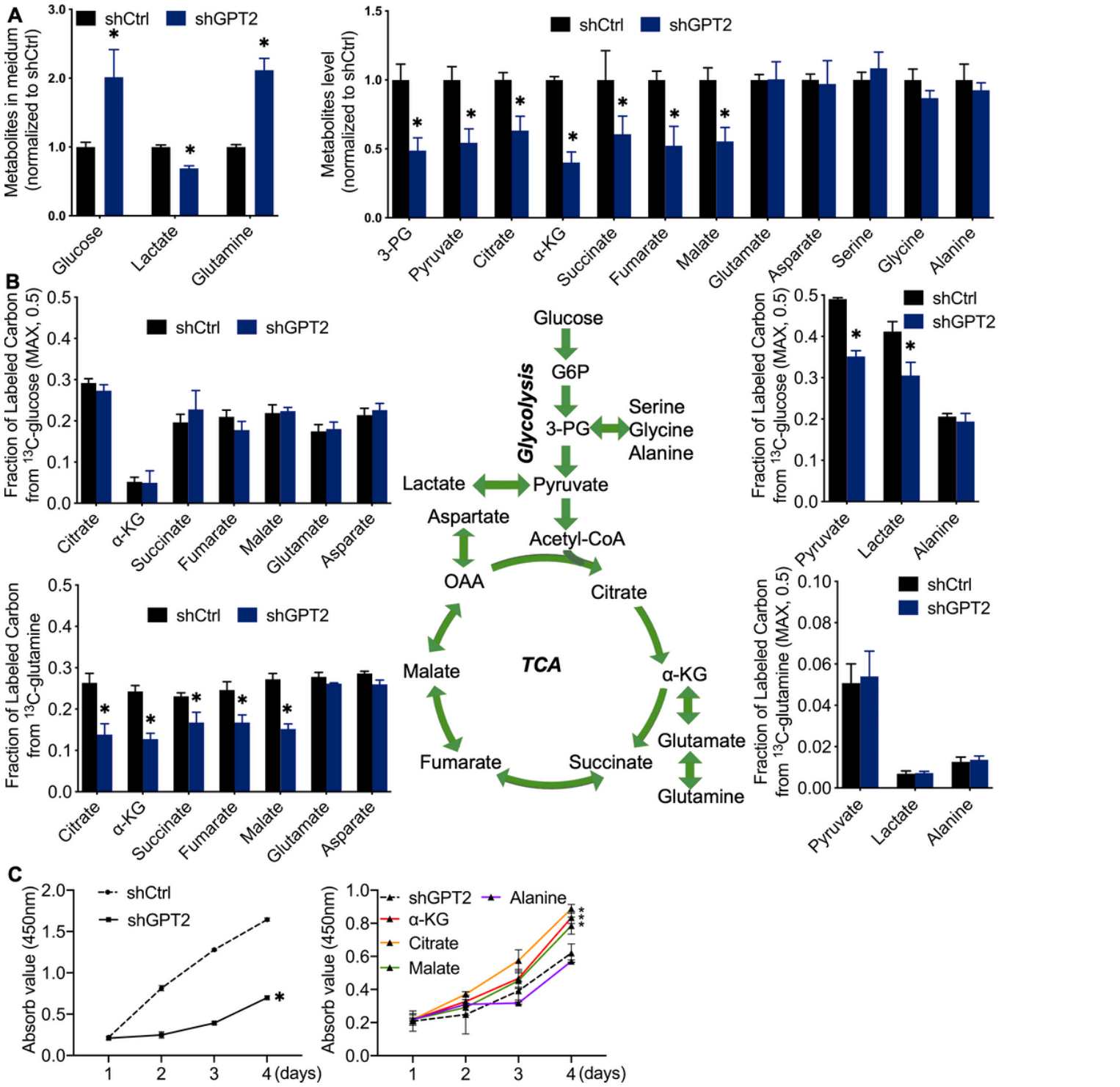

Figure 5

The metabolic characteristics of GPT2 in glutamate-driven anaplerosis A, Glucose uptake, lactate secretion, glutamine uptake decreased by GPT2 knockdown in 5637 cells. Metabolites in culture medium and cellular metabolites levels examined by MS. Cells were grown in the medium for 24 hr, and metabolites levels were analyzed by MS and normalized to shCtrl group. B, Fraction of labelled metabolic intermediates during 13C glucose and 13C-glutamine tracing experiments. C, a-KG, citrate, or malate rescues 5637 cells from suppressed cell proliferation caused by shGPT2. Cells were grown in medium with the presence of the indicated nutrient. CCK8 assay was performed to determine the cell viability in 5637 cells for indicated times. n = 3 independent

samples. * P < 0.01 compared with shCtrl group. G6P, glucose-6-phosphate; 3-PG, D-glycerate 3-phosphate; OAA, oxaloacetate.